



# Fermi National Accelerator Laboratory

FERMILAB-Pub-75/25-EXP  
7100.186

(Submitted to Phys. Rev. Letters)

## EXCITATION OF HIGH ENERGY PROTONS INTO LOW MASS STATES IN p-d INTERACTIONS

Y. Akimov, L. Golovanov, S. Mukhin, G. Takhtamyshev, and V. Tsarev  
Joint Institute for Nuclear Research, Dubna, USSR

E. Malamud, R. Yamada, and P. Zimmerman  
Fermi National Accelerator Laboratory, Batavia, Illinois 60510 USA

R. Cool, K. Goulianos, and H. Sticker  
Rockefeller University, New York, New York 10021 USA

and

D. Gross, A. Melissinos, D. Nitz, and S. Olsen  
University of Rochester, Rochester, New York 14627 USA

April 1975



EXCITATION OF HIGH ENERGY PROTONS INTO LOW MASS STATES IN  
p-d INTERACTIONS\*

Y. Akimov, R. Cool, L. Golovanov, K. Goulianos, D. Gross,  
A. Melissinos, E. Malamud, S. Mukhin, D. Nitz, S. Olsen<sup>†</sup>,  
H. Sticker, G. Takhtamyshev, V. Tsarev<sup>‡</sup>, R. Yamada and P. Zimmerman<sup>§</sup>

Fermi National Accelerator Laboratory, Batavia, Illinois 60510  
Joint Institute for Nuclear Research, Dubna, U.S.S.R.  
Rockefeller University, New York, New York 10021  
University of Rochester, Rochester, New York 14627

We have measured p-d inelastic scattering at small momentum transfer by detecting the slow recoil deuterons from a deuterium gas jet target. The coherent diffraction dissociation of protons on deuterons was studied in the region  $0.03 < |t| < 0.07$  (GeV/c)<sup>2</sup>,  $1.4 < M_x^2 < 4$  (GeV)<sup>2</sup>, and for energies from 50 to 275 GeV. In this region, the diffractive cross-section exhibits structure and is dominated by an enhancement at  $M_x^2 \sim 1.9$  (GeV)<sup>2</sup>.

---

\* Work supported in part by the U. S. Energy Research and Development Administration under Contracts AT(11-1)-2232A and AT(11-1)-3065, and by the U.S.S.R. State Committee for Atomic Energy.

<sup>†</sup> Alfred P. Sloan Foundation Fellow

<sup>‡</sup> Present Address: P. N. Lebedev Institute, Moscow, U.S.S.R.

<sup>§</sup> Present Address: Louisiana State University, Baton Rouge, Louisiana 70803

In an experiment performed at the Fermi National Accelerator Laboratory we studied the coherent inclusive reaction



at small momentum transfer<sup>(1)</sup>. Here we report results in the range  $m_p^2 < M_x^2 < 4 \text{ (GeV)}^2$  which covers several of the known resonant states of the proton. Data were obtained at incident energies of 50, 180 and 275 GeV. Excitation to states of higher mass is reported in the following letter<sup>(2)</sup>.

The target consisted of a deuterium gas jet<sup>(3)</sup> placed in the internal beam of the accelerator. The slow recoil deuterons were detected by stacks of two silicon solid state detectors (surface barrier) of thickness typically 200  $\mu\text{m}$  for the front and 1500  $\mu\text{m}$  for the rear detector. Only recoils stopping in the rear detector were accepted, and deuterons were unambiguously identified by the energy deposited in each detector. This technique limits the four-momentum transfer that could be measured to the range<sup>(4)</sup>

$0.03 \leq |t| \leq 0.07 \text{ (GeV/c)}^2$ . The detectors were mounted near  $90^\circ$  with respect to the beam direction on a movable carriage at a distance of 2.5m from the target and each stack subtended a solid angle  $\Delta\Omega \sim 16 \times 10^{-6}$  steradians.

The detection technique of slow recoils from high energy collisions has been previously used for the measurement of p-p elastic<sup>(5)</sup> and inelastic<sup>(6)</sup> scattering as well as for p-d elastic scattering<sup>(7)</sup>. A description of the apparatus and method is given in ref. (8) which discusses the measurement of elastic p-d scattering by the authors of this letter.

At a fixed recoil angle  $\omega$  (measured from  $90^\circ$ ) the mass  $M_x^2$  is given by

$$M_x^2 = m_p^2 + 2p \left[ \sin \omega \sqrt{|t|} - \frac{m_d + p}{2p m_d} |t| \right] \quad (2)$$

where  $p$  is the incident momentum and  $|t|$ , the four-momentum transfer, is given by

$$|t| = 2m_d T \quad (3)$$

with  $T$  the kinetic energy of the recoil deuteron. The data were normalized by using a fixed detector stack which measured elastic scattering at  $|t| = 0.043 \text{ (GeV/c)}^2$ . The elastic p-d cross-section was taken to be<sup>(8)</sup>

$$\left. \frac{d\sigma}{dt} \right|_{el} = \frac{(\sigma_{\tau}^{pd})^2}{16\pi} (1 + \rho^2) e^{-b|t|} + c t^2 \quad (4)$$

with  $\sigma_{\tau}^{pd}$  the total pd cross-section and  $\rho$  the ratio of real to imaginary part of the forward elastic scattering amplitude. Details are discussed in ref. (8). We believe that the uncertainty in normalization is smaller than  $\pm 3\%$ .

The resolution in  $M_x^2$  is dominated by the uncertainty in the recoil angle,  $\Delta\omega$ . Detector size and the width of the jet limit  $\Delta\omega$  to about  $\pm 3$  mrad. It holds that

$$\Delta M_x^2 = 2p \sqrt{|t|} \Delta\omega \quad (5)$$

In order to improve the mass resolution, especially at the higher incident momenta, we used a slit to limit the extent of the jet target (along the beam direction) seen by a particular detector. This reduced  $\Delta\omega$  to  $\pm 1.2$  mrad. Furthermore, slit scattering was monitored by running a jet at low energy (50 GeV)

where essentially no inelastic protons are produced over the useful kinetic energy range covered by the detector. Since the elastic scattering is so dominant, the bulk of the slit-scattered deuterons originate from the elastic peak which is (practically) independent of the incident energy. Thus the 50 GeV slit data could be used as a measure of the background present at higher energies. Use of the slit is limited to  $M_x^2 \leq 4 \text{ GeV}^2$  because, to assure proper normalization, each detector must also monitor elastic scattering (i.e., be located at small angles).

An additional contribution to the mass resolution arises from the uncertainty in the incident momentum,  $p$ . In this case

$$\Delta M_x^2 = \frac{\Delta p}{p} (M_x^2 - m_p^2) . \quad (5a)$$

The 50 GeV cross-sections were determined without the slit and typically  $\Delta\omega = \pm 3 \text{ mrad}$ , but  $\Delta p = \pm 1 \text{ GeV}$ . The 180 and 275 GeV data were taken with the slit so that  $\Delta\omega = \pm 1.2 \text{ mrad}$  but  $\Delta p = \pm 8 \text{ GeV}$ . On the average,  $\Delta M_x^2 = \pm 0.07 \text{ (GeV)}^2$ .

In Fig. 1, we show typical differential cross-sections at masses  $M_x^2 = 1.9, 2.7$  and  $3.1 \text{ GeV}^2$ , for 275 GeV incident energy. These cross-sections exhibit a steep  $t$ -dependence as expected for coherent scattering from deuterons. We find no evidence for a turnover in the  $t$ -distributions down to values of  $|t| \approx 0.03 \text{ (GeV/c)}^2$ . Within our  $t$ -range, these distributions could be fitted by single exponentials. However, since the deuteron form factor,  $S(t)$ , determined from elastic scattering can be expressed (for small values of  $t$ ) in the form<sup>(7,8)</sup>

$$|S(t)|^2 = e^{-b_0|t|} + c_0 t^2 \quad (6)$$

with (8)  $b_0 = 26.4 \text{ (GeV/c)}^{-2}$  and  $c_0 = 62.3 \text{ (GeV/c)}^{-4}$ , we have fitted the differential cross-sections with a form similar to Eq. (6)

$$\frac{d^2\sigma}{dt dM_x^2} = A e^{-b_d[|t| - 0.035]} + c_0[t^2 - (0.035)^2] \quad (7)$$

The parameters A and  $b_d$  were obtained from the fit, while  $c_0$  was fixed at  $c_0 = 62.3 \text{ (GeV/c)}^{-4}$ . The fit was made around the central value of our measured t-range,  $|t| = 0.035 \text{ (GeV/c)}^2$ , so that the best fit values and errors of A and  $b_d$  remain uncorrelated.

The results of the fits for  $d^2\sigma/dtdM_x^2$  at  $|t| = 0.035$  are given in Table I as a function of  $M_x^2$  and shown in Fig. 2. We note the existence of a prominent broad enhancement in the region  $M_x^2 \approx 1.9 \text{ (GeV)}^2$  and a smaller peak at  $M_x^2 = 2.8 \text{ GeV}^2$  which we identify with the  $N^*(1688)$  state. In Table I we also give average values for  $b_d$ . If it is assumed that the deuteron cross-sections factorize as  $d\sigma(pd) = d\sigma(pp) \cdot F_d$ , where  $F_d(t)$  is the coherence factor defined as

$$F_d(t) = \left( \frac{\sigma_{\tau}^{pd}}{\sigma_{\tau}^{pp}} \right)^2 |S(t)|^2, \quad (8)$$

then  $b_N \equiv (b_d - b_0)$  is a measure of the "slope-parameter" for the diffractive dissociation of the proton on a nucleon<sup>(9)</sup>. We note that if  $b_0$  is treated

as a constant independent of  $M_x^2$ , the slope parameter  $b_N$  decreases from a value of  $b_N \approx 24 \text{ (GeV/c)}^{-2}$  at  $M_x^2 \approx 1.9 \text{ (GeV)}^2$  to  $b_N \approx 10 \text{ (GeV/c)}^{-2}$  at  $M_x^2 \approx 4.0 \text{ (GeV)}^2$ .

In order to compare these data with previously known results on the diffractive excitation of the proton we have divided the differential cross-section by  $F_d(t)$  evaluated at the appropriate  $t$ -value. If the cross-section factorizes, this procedure should yield the corresponding data for  $pp \rightarrow Xp$ . In Fig. 3 we show data for this reaction obtained<sup>(10)</sup> at 20 GeV, together with our 50 GeV and 275 GeV data refit about the corresponding central  $t$ -value of  $0.042 \text{ (GeV/c)}^2$ . In Figs. 4a and 4b, we compare our results with data for the reaction  $pp \rightarrow Xp$  obtained<sup>(6)</sup> at 175 and 260 GeV, where the central  $t$ -value used is  $0.025 \text{ (GeV/c)}^2$ . The agreement between the high energy results indicates that the cross-section does indeed factorize. We further observe that the general behavior of the low-mass diffractive excitation of the proton does not change its character between 20 and 300 GeV, even though the overall cross-section decreases markedly with energy. If one assumes the presence of a background, as discussed in ref. (10), the magnitude of the 1400 enhancement peak changes very little with energy. The changing values of  $b_N$  and the structure in the cross-section as a function of  $M_x^2$  are distinctly different from the smooth behavior for  $M_x^2 > 5 \text{ GeV}^2$  reported<sup>(2)</sup> in the following letter.

We are grateful to many members of the Fermilab staff and in particular to the personnel of the Internal Target Section for their cooperation in the planning and execution of this experiment. We acknowledge the support of the technical staff at Rockefeller University and the University of Rochester. The Soviet members of our team express their gratitude to the State Committee for Atomic Energy of the USSR and the JINR, Dubna, for their generous support.

REFERENCES AND NOTES

1. Preliminary results from this experiment were reported at the XVII<sup>th</sup> International Conference on High Energy Physics, London (1974). See Y. Akimov et al, NAL-Conf-74-56 EXP and NAL-Conf-74-66 EXP.
2. Y. Akimov et al., Phys. Rev. Letters (following letter).
3. V. Bartenev et al., Adv. Cryog. Eng. 18, 460 (1973).
4. By the use of a 5mm lithium drifted detector as the 2<sup>nd</sup> detector of a stack, the t-range was extended to  $|t| \approx 0.12 \text{ (GeV/c)}^2$  in some cases.
5. Y. Akimov et al., J. Exptl. Theoret. Phys. (USSR) 48, 767 (1965). Translated JETP 21, 507 (1965); Y. Akimov et al., J. Nucl. Phys. (USSR) 4, 88 (1966). Translated JNP 4, 88 (1967). V. Bartenev et al., Phys. Rev. Letters 31, 1088 (1973) and 31, 1367 (1973) and references given in these papers.
6. V. Bartenev et al., Phys. Letters 51B, 299 (1974).
7. L. S. Zolin et al, J. Nucl. Phys. (USSR) 18, 30 (1974).
8. Y. Akimov et al., "Proton Deuteron Elastic Scattering at Small Momentum Transfer from 50 to 400 GeV/c," submitted for publication to Phys. Rev.
9. We point out that, although  $b_0$  as extracted from elastic scattering is strongly correlated to  $c_0$ , the values for  $b_N$  and for the extracted nucleon cross-sections are not affected by variations of the parameters  $b_0$  and  $c_0$  within the constraint imposed by the elastic scattering data (refs. 7 and 8).
10. R. M. Edelstein et al., Phys. Rev. D5, 1073 (1972).



TABLE I

The results of the fit to the data using the form given in equation 7.

$P_{lab} \rightarrow$	50 GeV/c	180 GeV/c	275 GeV/c
$M_x^2$			
$(GeV)^2$	$\frac{d^2\sigma}{dt dM_x^2} \Big _{ t =0.035}$ mb $\cdot (GeV/c)^{-2} \cdot GeV^{-2}$	$\frac{d^2\sigma}{dt dM_x^2} \Big _{ t =0.035}$ mb $\cdot (GeV/c)^{-2} \cdot GeV^{-2}$	$\frac{d^2\sigma}{dt dM_x^2} \Big _{ t =0.035}$ mb $\cdot (GeV/c)^{-2} \cdot GeV^{-2}$
	$b$ (GeV/c) $^{-2}$	$b$ (GeV/c) $^{-2}$	$b$ (GeV/c) $^{-2}$
1.35		1.88 ± .29	3.29 ± .24
1.45		2.47 ± .29	3.13 ± .14
1.55	5.55 ± .26	2.83 ± .20	3.75 ± .15
1.65	6.60 ± .23	3.71 ± .14	
1.75	6.87 ± .36	4.38 ± .15	5.01 ± .25
1.85	8.52 ± .39	5.09 ± .14	4.67 ± .14
1.95	9.11 ± .47	4.86 ± .16	4.87 ± .15
2.05	7.65 ± .44	4.72 ± .23	4.68 ± .33
2.15	6.34 ± .40	4.26 ± .19	4.37 ± .21
2.25	5.89 ± .71	3.78 ± .16	3.74 ± .12
2.35	5.72 ± .47	3.24 ± .12	3.18 ± .14
2.45	5.05 ± .43	2.78 ± .17	3.09 ± .11
2.55	4.74 ± .69	3.04 ± .16	2.73 ± .12
2.65	6.07 ± .51	2.85 ± .17	2.86 ± .16
2.75	5.48 ± .73	3.48 ± .19	2.75 ± .17
2.85	5.27 ± .45	3.27 ± .41	2.64 ± .13
2.95	3.39 ± .34	3.22 ± .20	2.60 ± .16
3.05	3.59 ± .28	2.71 ± .20	2.04 ± .10
3.15	2.71 ± .30		1.87 ± .10
3.25	2.55 ± .21		1.89 ± .15
3.35	2.23 ± .21		1.47 ± .10
3.45	2.24 ± .25		1.38 ± .12
3.55	1.76 ± .22		1.30 ± .17
3.65	1.58 ± .20		1.38 ± .12
3.75	1.91 ± .41		1.37 ± .10
3.85	2.13 ± .37		1.29 ± .11
3.95	1.95 ± .38		1.35 ± .10
	37.2 ± 7.2	43.6 ± 3.6	49.1 ± 2.3
	40.1 ± 2.2	50.4 ± 1.6	48.2 ± 1.7
	43.4 ± 5.4	41.8 ± 2.4	43.4 ± 2.4
	41.7 ± 4.4	39.9 ± 3.2	40.7 ± 2.0
	36.1 ± 4.1		38.5 ± 2.8
	32.8 ± 4.4		35.0 ± 4.5

φ

FIGURE CAPTIONS

1. Differential cross-sections at 275 GeV/c vs.  $t$  for  $M_x^2 = 1.9, 2.7$  and  $3.1 \text{ (GeV)}^2$ .
2. Values of  $(d^2\sigma/dtdM_x^2)$  at  $|t| = 0.035 \text{ (GeV/c)}^2$  vs.  $M_x^2$  for incident energies of 50, 180 and 275 GeV.
3. A comparison of our results for  $(1/F_d) (d^2\sigma/dtdM_x^2)|_{|t| = .042}$  at 50 and 275 GeV with the 20 GeV pp results reported in ref. 10. The curve is a fit reported in ref. 10 including resonances and a "non resonant" background.
4. a) A comparison of  $(1/F_d) (d^2\sigma/dtdM_x^2)|_{|t| = .025}$  at 180 GeV with 175 GeV pp data (ref. 6);  
b) A similar comparison of our 275 GeV data with the 260 GeV data of ref. 6.

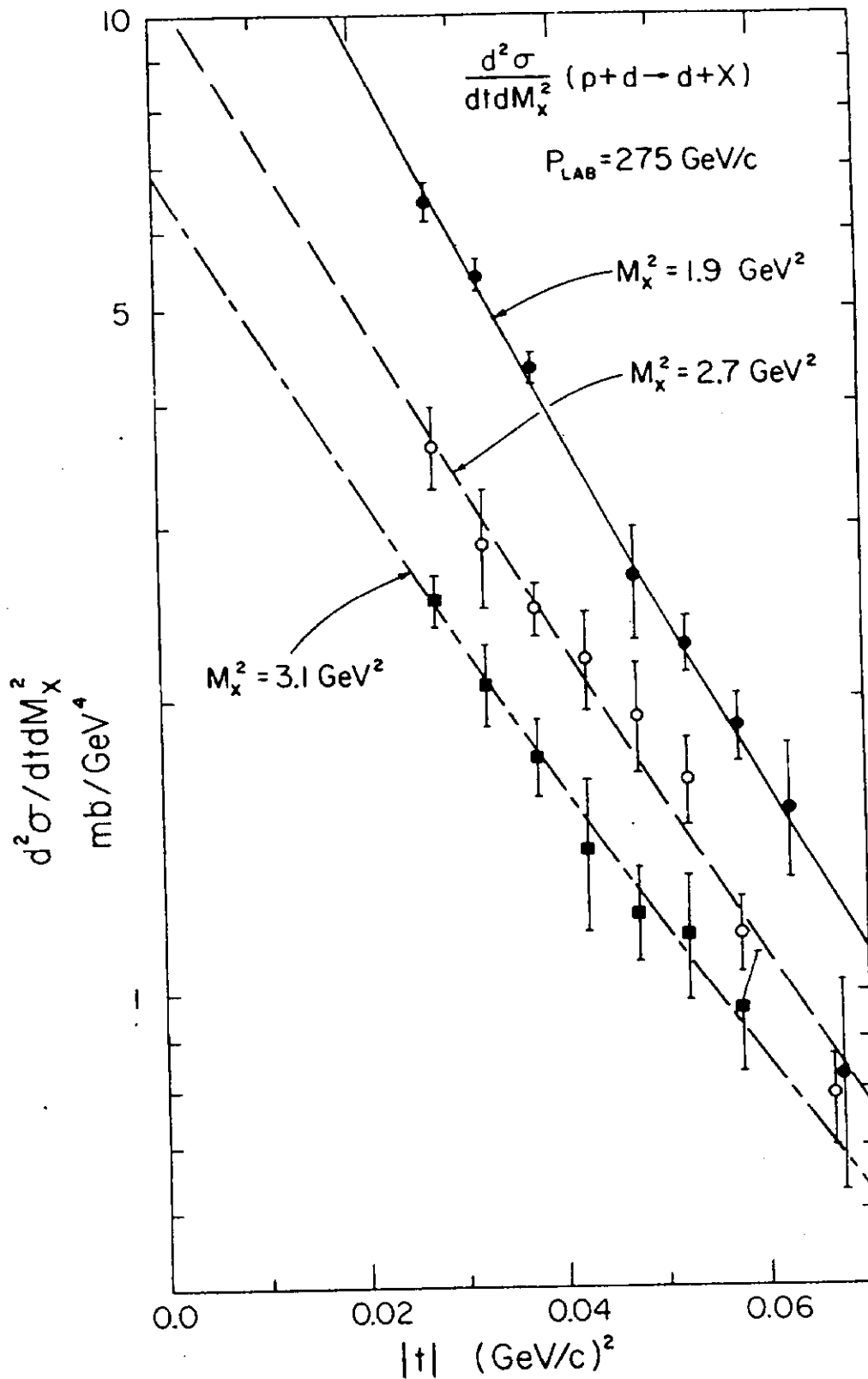


Fig. 1

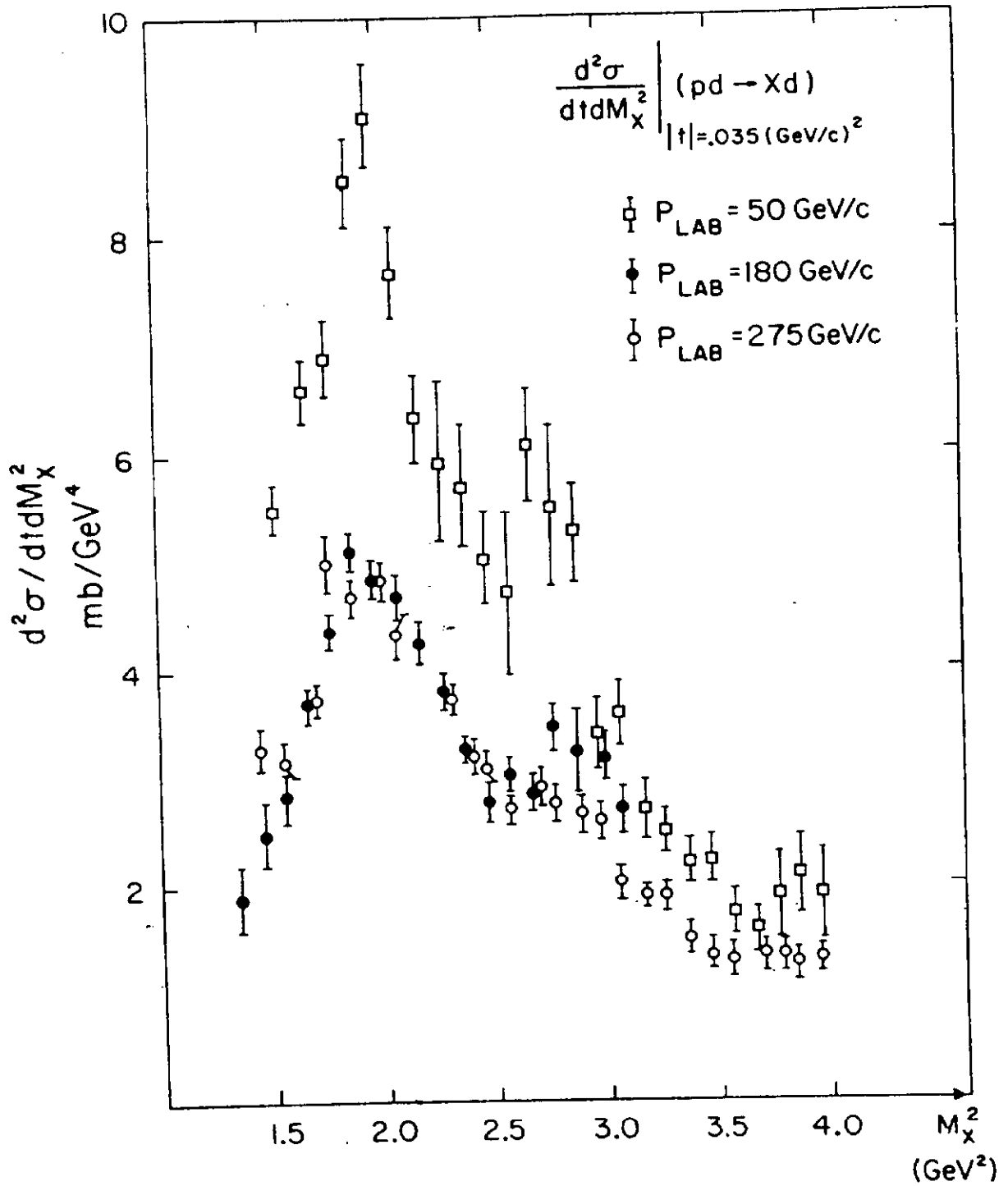


Fig. 2

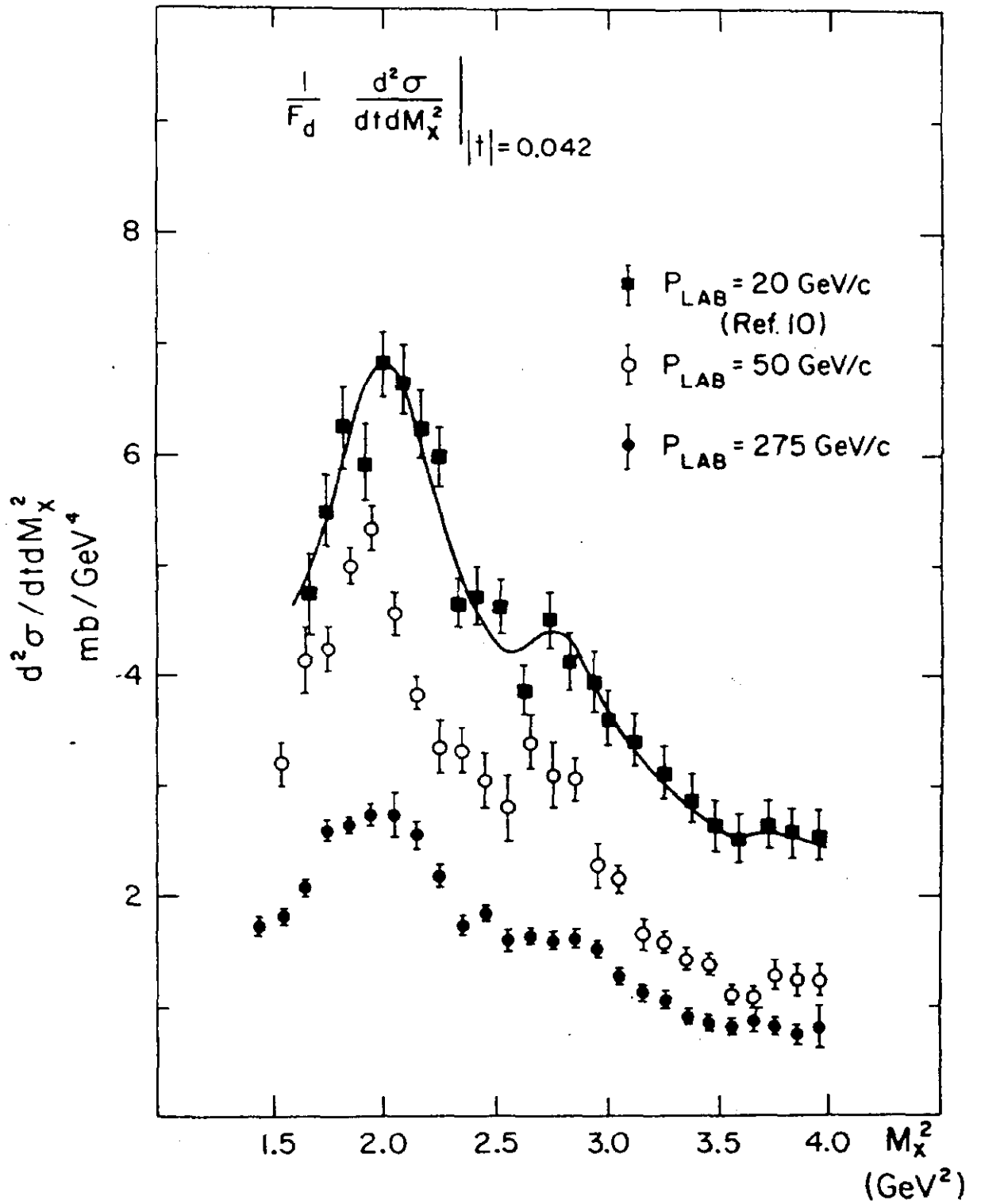


Fig. 3

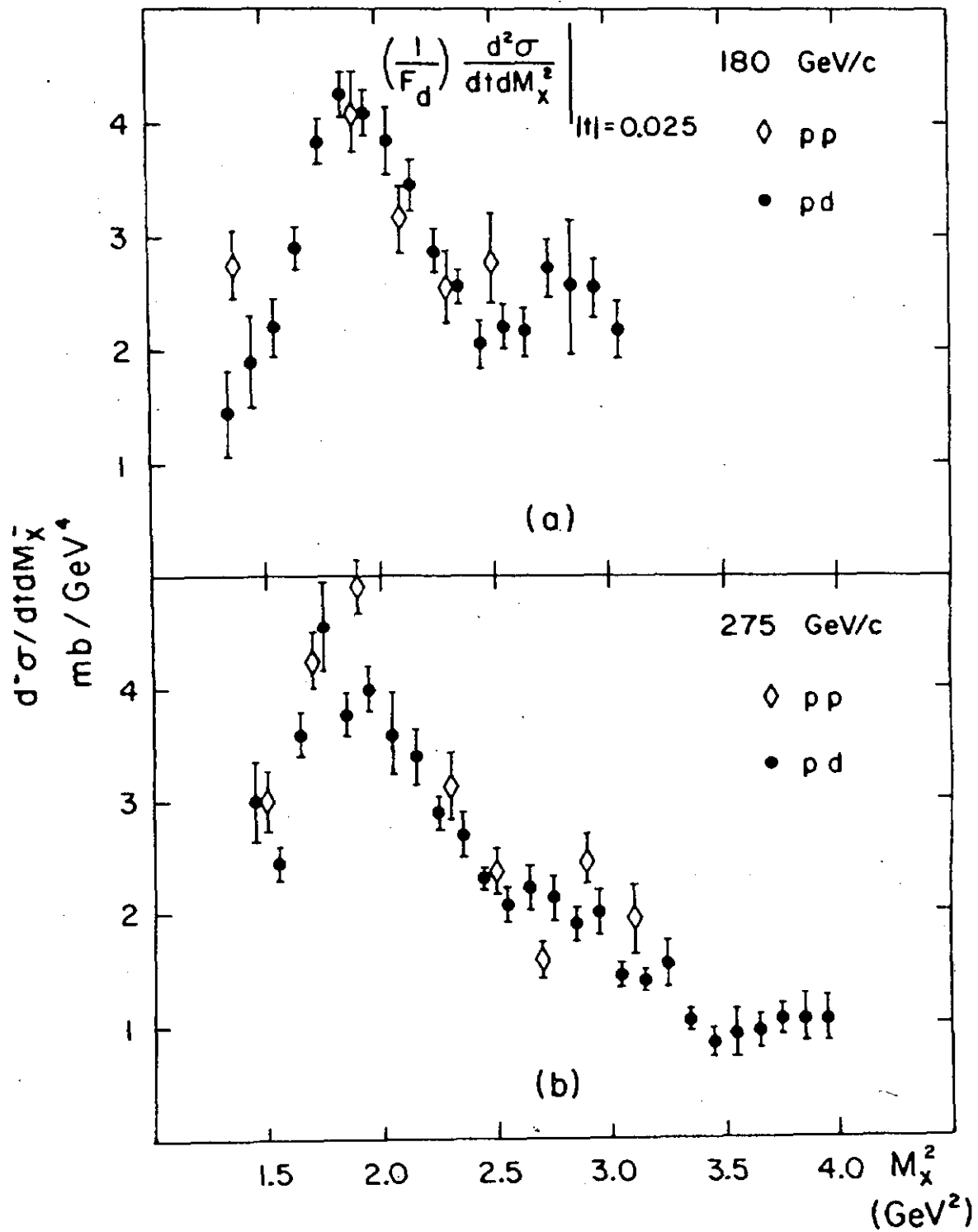


Fig. 4